

# Etching materials with an atmospheric-pressure plasma jet

J Y Jeong<sup>†</sup>, S E Babayan<sup>†</sup>, V J Tu<sup>†</sup>, J Park<sup>‡</sup>, I Henins<sup>†</sup>,  
R F Hicks<sup>†§</sup> and G S Selwyn<sup>‡</sup>

<sup>†</sup> Chemical Engineering Department, University of California, Los Angeles,  
CA 90095-1592, USA

<sup>‡</sup> Plasma Physics, Los Alamos National Laboratory, Los Alamos, NM 87545, USA

Received 13 November 1997, in final form 9 March 1998

**Abstract.** A plasma jet has been developed for etching materials at atmospheric pressure and between 100 and 275 °C. Gas mixtures containing helium, oxygen and carbon tetrafluoride were passed between an outer, grounded electrode and a centre electrode, which was driven by 13.56 MHz radio frequency power at 50 to 500 W. At a flow rate of 51 l min<sup>-1</sup>, a stable, arc-free discharge was produced. This discharge extended out through a nozzle at the end of the electrodes, forming a plasma jet. Materials placed 0.5 cm downstream from the nozzle were etched at the following maximum rates: 8.0 μm min<sup>-1</sup> for Kapton (O<sub>2</sub> and He only), 1.5 μm min<sup>-1</sup> for silicon dioxide, 2.0 μm min<sup>-1</sup> for tantalum and 1.0 μm min<sup>-1</sup> for tungsten. Optical emission spectroscopy was used to identify the electronically excited species inside the plasma and outside in the jet effluent.

Atmospheric-pressure plasmas, such as the thermal torch, plasma arc, corona discharge and silent discharge, have been the focus of much research. This is motivated by the growing need for new chemical and materials processing technologies. Thermal torches and arcs are high-temperature sources (>10 000 °C) that are used for a variety of materials applications, including melting and deposition, spray coating and ceramic powder synthesis [1–4]. Corona and silent discharges operate at much lower gas temperatures, between 25 and 500 °C [5, 6]. The corona discharge uses one or more sharply curved electrodes (e.g., spheres, or wires), so that the plasma is confined to a small region near the electrode [7–9]. The silent discharge consists of two closely spaced electrodes that are covered with dielectric layers [10–14]. This plasma generates many microscopic discharges that last only a few nanoseconds, and are randomly distributed in space and time. Since the corona and silent discharges do not uniformly treat large substrate areas, they are not well suited for materials processing.

Five years ago, Koinuma *et al* [11] introduced a micro-beam plasma for etching materials. This device operates by ionizing a gas that flows between two closely spaced concentric electrodes separated by a quartz tube. A profile of silicon etched with a 1.0 volume percent CF<sub>4</sub>/He plasma reveals a narrow trench (0.15 μm in width) with straight sidewalls, indicating directional etching by ions.

Herein, we report on the design and operation of an atmospheric-pressure plasma jet. This source is

§ Corresponding author: rhicks@ucla.edu

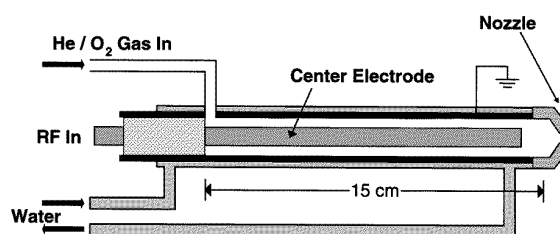


**Figure 1.** Schematic of the atmospheric-pressure plasma jet. Drawing approximately to scale.

different from those described above, because it produces a uniform plasma at low temperature that may be used for materials processing on relatively large substrates. Below, we describe the application of the jet for etching materials.

A schematic of the plasma jet is shown in figure 1. It consists of an inner electrode, which is coupled to a radio-frequency power source at 13.56 Mhz, and a grounded outer electrode. A mixture of helium and other reactive gases is fed into the annular space between the two electrodes at 51 l min<sup>-1</sup> (at 760 Torr and 293 K). To etch organic films, oxygen is added to the helium carrier gas. To etch silicon dioxide and metals, carbon tetrafluoride is added in addition to the oxygen. A soft white glow is produced between the electrodes (for O<sub>2</sub> and He), which then exits the device through a nozzle at 30 m s<sup>-1</sup>. Outside the device, the gas is at the prevailing atmospheric pressure, and there is no significant pressure drop across the nozzle. Samples are etched by placing them at 0.5 cm from the nozzle. An

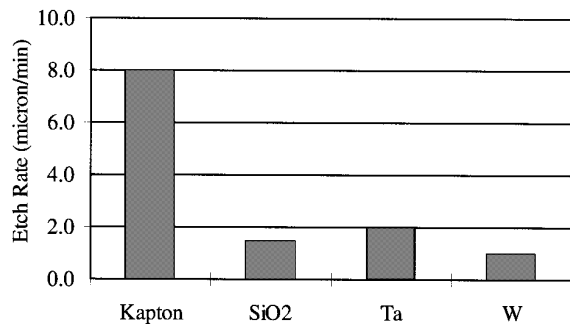


**Figure 2.** Etching rates achieved with the plasma jet. For Kapton etching: 51 l min<sup>-1</sup> helium flow, 1.2% O<sub>2</sub> and 500 W. For SiO<sub>2</sub> W and Ta: 51 l min<sup>-1</sup> helium flow, 1.0% O<sub>2</sub>, 2.0% CF<sub>4</sub> and 500 W.

aluminium mask is placed over the sample to restrict the area etched to 0.7 cm<sup>2</sup>.

Visual inspection of the discharge between the electrodes reveals a uniform glow with no apparent arcing. The window of stable operation is: helium flow rates greater than 25 l min<sup>-1</sup>, oxygen concentrations of up to 3.0% by volume, carbon tetrafluoride concentrations of up to 4.0% by volume, and RF power between 50 and 500 W. Helium is essential for obtaining a stable discharge. In addition, if the power is too high, or the flow rate too low, arcing occurs at the end of the centre electrode.

Shown in figure 2 are the rates at which the atmospheric-pressure plasma jet etches different materials. These rates were measured by weighing the films before and after exposure to the plasma jet effluent for a given time period. The plasma jet etched Kapton at 8.0 μm min<sup>-1</sup>, which is fast compared to a low-pressure plasma system [15–18]. Also, silicon dioxide, tantalum and tungsten are etched with a CF<sub>4</sub>/O<sub>2</sub>/He plasma jet at rates of 1.2, 2.0 and 1.0 μm min<sup>-1</sup>, respectively. The etching conditions for each material are given in the figure caption. In addition, good selectivity is achieved with the APPJ: an O<sub>2</sub>/He plasma jet etches Kapton and organic materials only, whereas a CF<sub>4</sub>/He plasma jet only etches SiO<sub>2</sub>, Ta and W.

To estimate the charged particle flux in the jet effluent, a planar probe was placed 0.5 cm away from the centre of the nozzle. An ion flux of 5 × 10<sup>13</sup> particles cm<sup>-2</sup> s<sup>-1</sup> was collected on the probe when it was negatively biased by 100 V to the floating potential. In this experiment, the RF power was 150 W, the helium flow rate was 40 l min<sup>-1</sup> and the gas containing 0.5% oxygen by volume. A Kapton etch rate of 0.4 μm min<sup>-1</sup> is observed for these operating conditions. This etch rate is several orders of magnitude higher than that expected for the ion flux observed with the Langmuir probe [19]. Also, biasing a tantalum foil at -200 V does not lead to any enhancement of the etch rate. These results indicate that ions do not participate in the etching process.

Optical emission spectroscopy has been used to observe the electronically excited species generated by the O<sub>2</sub>/He plasma jet. In figure 3(a), an emission spectrum of the discharge between the two electrodes is shown. The process

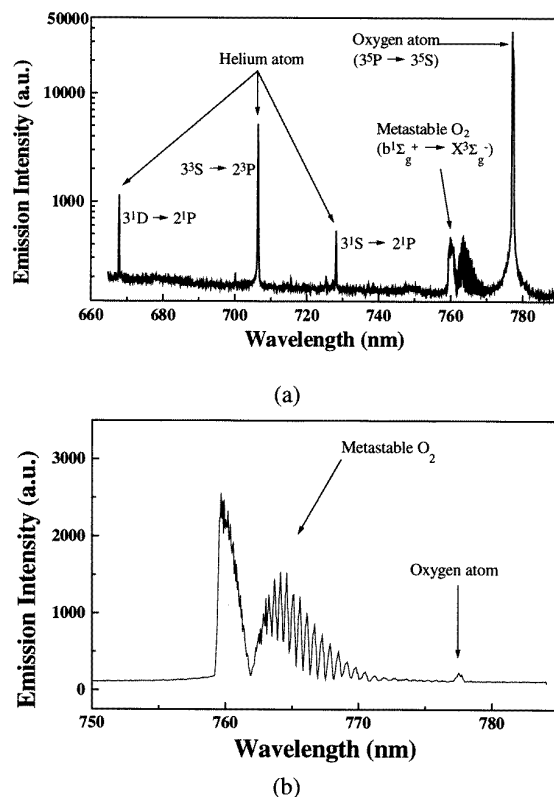


**Figure 3.** Optical emission spectra of an O<sub>2</sub>/He atmospheric pressure plasma jet taken (a) axially inside the jet, exposure time = 0.5 second, and (b) perpendicularly outside the jet, exposure time = 2 min.

conditions are 150 W RF power, 0.5% oxygen by volume and 42 l min<sup>-1</sup> helium (at 25 °C and 760 Torr). In addition, the nozzle of the jet was removed to better view axially along the electrodes. Examination of the spectrum reveals atomic helium lines at 667.8, 706.5 and 728.2 nm, an atomic oxygen line at 777.2 nm, and singlet sigma metastable oxygen (b<sup>1</sup>Σ<sub>g</sub><sup>+</sup>) at 758–770 nm [20]. Spectra obtained over different wavelength ranges contain more atomic helium lines at 447.1, 501.6, 587.6 and 656.0 nm, and more atomic oxygen lines at 436.8, 533.1, 615.8, 645.6, 794.8, 822.2 and 844.6 nm. Furthermore, a weak band for molecular oxygen ion is seen at 580–640 nm (first negative system).

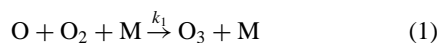
In figure 3(b), a spectrum is shown of the plasma jet effluent, taken perpendicular to the flow direction. To prevent reflected interference from the emission inside the jet, a slit and a lens were used to focus on the effluent at 4.0 mm from the nozzle. It is evident from the figure that the emission from excited atoms and ions is nearly extinct. The only distinguishable feature is the band between 757 and 773 nm, which is due to the transition from singlet sigma metastable oxygen to ground state oxygen. These results can be explained by the absence of an excitation source in the jet effluent. The atoms and ions have radiative de-excitation times of ~10 ns [21], and relax to the ground state immediately upon exiting the nozzle. On the other hand, the singlet sigma metastable oxygen molecules

exhibit a much longer lifetime of  $\sim 100 \mu\text{s}$  [22]. For a flow velocity of  $30 \text{ m s}^{-1}$ , the gas travels 4 mm to the detection point in  $130 \mu\text{s}$ .

Preliminary infrared emission measurements at  $1.27 \mu\text{m}$  indicate that singlet delta metastable oxygen ( $a^1\Delta_g$ ) is present in the jet effluent. Moreover, this species persists for up to 10 cm from the nozzle. This is a result of its exceptionally long lifetime,  $\tau_{1/2} \sim 100 \text{ ms}$  [22]. Other researchers have estimated that in low-pressure plasma discharges, the concentration of singlet delta should be greater than the sigma state by two to three orders of magnitude [23–25]. It is well documented that the metastable oxygen molecules ( $a^1\Delta_g$  and  $b^1\Sigma_g^+$ ) are capable of oxidizing organic compounds [23]. Therefore, these species could participate in the Kapton etching reaction.

An electrochemical ozone detector (Gas Tech SC-90) was used to measure the amount of ozone present in the jet effluent. Ozone is known for its high reactivity with organic materials, and is often used in combination with UV irradiation for photoresist etching [26]. However, ozone probably does not contribute significantly to the etching rate achieved with the atmospheric-pressure plasma jet. For example, at 200 W, 0.8%  $\text{O}_2$  by volume and  $51 \text{ l min}^{-1}$  helium flow, the  $\text{O}_3$  concentration varies from 27 to 56 ppm at 0.6 to 3.8 cm from the nozzle. This amount of ozone is not sufficient to achieve an appreciable etching rate of Kapton [26].

Based on the ozone concentration, one can estimate the concentration of oxygen atoms in the plasma jet. The two main reactions involving oxygen atoms and ozone are:



Values for the rate constants  $k_1$  and  $k_2$  at  $100^\circ\text{C}$  are  $3.6 \times 10^{-34} \text{ cm}^6 \text{ molecule}^{-2} \text{ s}^{-1}$  and  $3.2 \times 10^{-14} \text{ cm}^3 \text{ molecule}^{-1} \text{ s}^{-1}$ , respectively [27]. Assuming ideal plug flow in the jet, the mass balance for ozone is:

$$v_z \frac{d[\text{O}_3]}{dz} = k_1[\text{O}][\text{O}_2] \cdot \beta[\text{M}] - k_2[\text{O}][\text{O}_3]. \quad (3)$$

In this equation,  $v_z$  is the flow velocity ( $30 \text{ m s}^{-1}$ );  $z$  is the distance downstream from the nozzle (m);  $[\text{O}]$ ,  $[\text{O}_2]$  and  $[\text{O}_3]$  are the concentrations of O atoms,  $\text{O}_2$  molecules and  $\text{O}_3$  molecules ( $\text{molecules cm}^{-3}$ );  $[\text{M}]$  is the gas pressure, equal to  $P/RT$  ( $\text{molecules cm}^{-3}$ ) and  $\beta$  is the ratio of the collision efficiency of helium to that of air at  $100^\circ\text{C}$  (0.71) [28]. The ozone concentrations measured at 0.6 to 3.8 cm from the nozzle are used as boundary conditions to solve equation (3). The calculated value of the O atom concentration at 0.6 cm is 36 ppm. If every O atom colliding with the Kapton film goes on to react with it, this quantity of oxygen atoms is more than enough to account for the observed Kapton etching rate.

In conclusion, a plasma jet has been developed which can be used to etch a variety of materials at atmospheric pressure and between  $100$  and  $275^\circ\text{C}$ . Preliminary analysis of the gas composition suggests that etching proceeds by a chemical mechanism. In the case of Kapton films, the two

potential reactive species that have been identified so far are singlet delta metastable oxygen and oxygen atoms.

## Acknowledgments

This work was conducted under the auspices of the US Department of Energy, supported in part by funds provided by the University of California, and in part by funds provided by Basic Energy Sciences, Environmental Management Sciences Program and the Office of Science and Risk Policy (award No DE-F5607-96ER45621). The authors, JYJ and SEB, are grateful for fellowships from the UCLA Centre for Environmental Risk Reduction and the UC Toxic Substance Research and Teaching Program.

## References

- [1] Boulos M 1991 *IEEE Trans. Plasma Sci.* **PS-19** 1078
- [2] Sanders D 1990 *Handbook of Plasma Processing Technology* ed S M Rossmagel, J J Cuomo and W D Westwood (Park Ridge, NJ: Noyes) p 419
- [3] Fleddermann C B, Snyder H R and Gahl J M 1996 *IEEE Int. Conf. on Plasma Science (Abstracts) (Boston, MA 1996)* (New York: IEEE) p 146
- [4] Uhm H S and Hong S H 1997 *Proc. 1997 IEEE Int. Conf. on Plasma Science (San Diego, CA 1997)* (New York: IEEE) p 152
- [5] Van Brunt R J 1994 *IEEE Trans. Dielectr. Electr. Insul.* **1** 761–84
- [6] Sherman P B 1993 *Proc. IEEE Industry Application Soc. Annu. Meeting (Toronto, 1993)* vol 3 (New York: IEEE) pp 1669–85
- [7] Nasser E 1971 *Fundamentals of Gaseous Ionization and Plasma Electronics* (New York: Wiley-Interscience)
- [8] Goldman M and Goldman A 1978 *Gaseous Electronics* vol 1, ed M N Hirsh and H J Oskam (New York: Academic) pp 219–90
- [9] Sigmond R S and Golman M 1983 *Electrical Breakdown and Discharges in Gases* part B, ed E E Kunhardt and L H Luessen (New York: Plenum) pp 1–64
- [10] Yokoyama T, Kogoma M, Kanazawa S, Moriwaki T and Okazaki S 1990 *J. Phys. D: Appl. Phys.* **23** 374
- [11] Koinuma H, Ohkubo H, Hashimoto T, Inomata K, Shiraishi T, Miyanaga A and Hayashi S 1992 *Appl. Phys. Lett.* **60** 816
- [12] Okazaki S, Kogoma M, Uehara M and Kimura Y 1993 *J. Phys. D: Appl. Phys.* **26** 889
- [13] Nagorny V P, Drallos P J and Williamson W Jr 1995 *J. Appl. Phys.* **77** 3645
- [14] Sawada Y, Tamaru H, Kogoma M, Kawase M and Hashimoto K 1996 *J. Phys. D: Appl. Phys.* **29** 2539
- [15] Juan W H and Pang S W 1994 *J. Vac. Sci. Technol. B* **12** 422
- [16] Horiiko Y, Kubota K, Shindo H and Fukaswa T 1995 *J. Vac. Sci. Technol. A* **13** 801
- [17] Kuo Y 1993 *Japan. J. Appl. Phys.* **32** 179
- [18] Maruyama T, Fujiwara N, Shiozawa K and Yoneda M 1995 *J. Vac. Sci. Technol. A* **13** 810
- [19] Joubert O, Pelletier J and Arnal Y 1989 *J. Appl. Phys.* **65** 5096
- [20] Herzberg G 1934 *Nature* **133** 759
- [21] Wiese W L and G A Martin (eds) 1978 *Wavelengths and Transition Probabilities for Atoms and Atomic Ions* (Washington, DC: US Government Printing Office)
- [22] Ogryzlo E A 1978 *Singlet Oxygen: Reactions with Organic Compounds and Polymers* ed B Ranby and J F Rabek (London: Wiley)
- [23] Wayne R P 1985 *Singlet O<sub>2</sub>* vol 1, ed A A Frimer (Boca Raton, FL: Chemical Rubber Company) p 81

- [24] Ogryzlo E A 1975 *Singlet Oxygen* ed H H Wasserman and R W Murray (New York: Academic) p 35
- [25] Kearns D R 1971 *Chem. Rev.* **71** 395
- [26] Wood P C, Wydeven T and Tsujii O 1993 *Surface Chemical Cleaning and Passivation of Semiconductor Processing Symposium* ed G S Higashi, E A Irene and T Ohmi (Pittsburgh, PA: Materials Research Society) p 237
- [27] DeMore W B, Sander S P, Golden D M, Hampson R F, Kurylo M J, Howard C J, Ravishankara A R, Kolb C E and Molina M J (eds) 1992 *Chemical Kinetics and Photochemical Data for Use in Stratospheric Modeling* (Pasadena, CA: JPA)
- [28] Gardiner W C and Troe J 1984 *Combustion Chemistry* ed W C Gardiner Jr (New York: Springer)